

Magnetic phase diagram of Eu_2CuSi_3 derived from thermal expansion and magnetostriction studies

L. Wang,^{1,*} L. Wallbaum,¹ C. Koo,¹ C. D. Cao,² W. Löser,³ and R. Klingeler^{1,4}

¹*Kirchhoff Institute of Physics, Heidelberg University,
INF 227, 69120 Heidelberg, Germany*

²*Department of Applied Physics, Northwestern
Polytechnical University, Xian 710072, P.R. China*

³*Leibniz Institute for Solid State and Materials Research IFW Dresden,
Helmholtzstr. 20, 01069 Dresden, Germany*

⁴*Center for Advanced Materials, Heidelberg University,
INF 225, 69120 Heidelberg, Germany*

(Dated: February 28, 2022)

Abstract

Precise thermal expansion and magnetostriction studies of the intermetallic compound Eu_2CuSi_3 in the temperature range between 5 and 300 K are presented. A clear sign of magnetic second order phase transition at the ferromagnetic Curie temperature $T_C = 34$ K indicates strong magnetostructural coupling. Uniaxial thermal expansion data show a large anisotropy between the magnetic easy c -axis and the hexagonal ab -plane, which is associated with a strongly anisotropic magnetic coupling. A spin-reorientation regime as well as a non-uniform energy scale are indicated by Grüneisen analysis of the data at low temperatures. Anomalous contributions to the thermal expansion imply ferromagnetic correlations far above in zero magnetic field. The magnetic phase diagram is constructed, showing the evolution of short- and long-range magnetic order in magnetic fields up to 15 T. The anisotropic magnetic field effect yields anomalous magnetostrictive effects up to about 200 K.

PACS numbers:

INTRODUCTION

Ternary intermetallic compounds Ln_2CuSi_3 (Ln = rare earth) are of considerable interest because of their diverse types of magnetic ordering and associated complex interplay of structural, orbital, electronic, and magnetic degrees of freedom. [1–10] Most of the known members of this class crystallize in a hexagonal AlB_2 -type structure (space group $\text{P6}/\text{mmm}$) with random distribution of Cu and Si atoms on the B positions. [11] One exception is Er_2CuSi_3 , crystallizing in a tetragonal ThSi_2 -type structure. [11] The great diversity of magnetic ground states originates from correlations of the localized f -electrons of the rare-earth elements, which are coupled by the conduction electrons according to the Ruderman-Kittel-Kasuya-Yosida theory. Some compounds exhibit unusual transport properties, namely large negative magnetoresistance has been found in Eu_2CuSi_3 above the Curie temperature [7, 9], even up to $T \sim 100$ K, and a typical Kondo behavior has been found in Ce_2CuSi_3 [1, 4]. Unusual mass enhancement of Ce_2CuSi_3 [1] and Pr_2CuSi_3 [2] has been unveiled by studies on the electronic specific heat. Weak spin glass behavior coexisting with long range ferromagnetic order is observed in Pr_2CuSi_3 and Nd_2CuSi_3 . [2, 6] However, due to particular challenges in single crystal growth [12], anisotropic properties have been reported so far only for Ce_2CuSi_3 [4] and Eu_2CuSi_3 [9] while all other experimental data rest on polycrystalline samples.

Due to its half-filled shell in the $4f^7$ electronic configuration, Eu_2CuSi_3 has a particular role among the lanthanides-based series of ternary intermetallics. The Eu^{2+} -ions in Eu_2CuSi_3 do not follow the lanthanide contraction rule. [7, 9] Instead, unit cell volume and lattice parameters in Eu_2CuSi_3 are abnormally enlarged, similar to what is observed in the more frequently studied family R_2PdSi_3 . [13] Ferromagnetic order in Eu_2CuSi_3 evolves at $T_C = 34$ K. Above T_C , magnetization data show a magnetic moment of $(7.8 \pm 0.1)\mu_B/\text{Eu}$, i.e., a stable valence of 2+ of Eu-ions. The anisotropy of the electron spin resonance signal of divalent Eu^{2+} -ions proves appreciable short-range ferromagnetic correlations up to $T \sim 100$ K, i.e., far above T_C . [9] Below T_C , there is a sizeable magnetic anisotropy with the crystallographic c -axis being the easy magnetic axis. In the temperature regime around 10 to 20 K the magnetic anisotropy gradually vanishes most probably due to a spin reorientation. It may be expected that, similar to other intermetallic materials (e.g., $\text{HoNi}_2\text{B}_2\text{C}$ [14], $\text{Tb}_x\text{Gd}_{1-x}\text{Al}_2$ [15], $\text{Mo}_{5+y}\text{Si}_{3y}\text{B}_x$ [16]), that magnetic anomalies are tightly coupled with

lattice changes. However, no investigations of magneto-structural effects are known for Eu_2CuSi_3 or any other member of this class of materials. Therefore, the investigation of thermal expansion and magnetostriction on a Eu_2CuSi_3 single crystal will elucidate the interrelation of structural, magnetic, and electron degrees of freedom. In the present work, we investigate in detail of the uniaxial lattice distortions induced by the magnetic transition as well as the influence of external magnetic fields. A detailed magnetic phase diagram of Eu_2CuSi_3 focusing on the low temperature range up to 70 K is derived from the data.

EXPERIMENTAL

Eu_2CuSi_3 single crystals have been grown by the traveling-solvent floating-zone method as described in Ref. 12. The relative length changes $\Delta L_i/L_i$ along the crystallographic c - and a -directions were studied (as the a - and b -axes are crystallographically equivalent) on a cuboidal shaped crystal which dimensions are 1.831 mm ($\parallel a$), 3.408 mm ($\parallel b$), and 1.792 mm ($\parallel c$). The measurements were done by means of a three-terminal capacitance dilatometer. [17] For investigating the effect of magnetic fields, the length changes and the thermal expansion coefficients $\alpha_i = 1/L_i \cdot dL_i(T)/dT$ were studied in magnetic fields up to 15 T applied along the axis i , respectively. In addition, the field induced length changes $\Delta L_i(B)/L_i$ were measured at temperatures T from 5 K to 200 K in magnetic fields up to 15 T and the magnetostriction coefficients $\lambda_i = 1/L_i \cdot dL_i(B)/dB$ were derived.

THERMAL EXPANSION AND GRÜNEISEN SCALING

The temperature dependence of the uniaxial length changes in Eu_2CuSi_3 shows that magnetic order is associated with pronounced magnetoelastic effects (Fig. 1b) both along c and in the ab -plane. Accordingly, the volume significantly shrinks upon evolution of magnetic order and the volume thermal expansion coefficient $\beta = 2\alpha_a + \alpha_c$ displays a peak (Fig. 1a). Qualitatively, this implies positive hydrostatic pressure dependence dT_C/dp . In addition, there is a broad shoulder in β at around 15 K and the region of anomalous volume changes extends well above T_C . According to Ref. 18, the electronic (β_{el}) and phononic (β_{ph}) contributions to the thermal expansion coefficient can be described by

$$\beta_{el} = K_1 \cdot T^2 \quad (1)$$

$$\beta_{ph} = K_2 T \cdot D(\Theta_D/T) \quad (2)$$

with K_1 and K_2 being constants and D being the Debye function. The red solid lines in Fig. 1 show the results of the fitting procedure to the experimental data well above T_C . For the fitting of both the volume and the uniaxial expansion data, the same Debye temperature $\Theta_D = 425$ K independently obtained from analysing the specific heat of La_2CuSi_3 (data from Ref. 1) is used here to ensure the consistency of the procedure. [20] Quantitatively, the differences between the estimated non-magnetic lengths changes and the actual experimental data at $T = 5$ K amounts to $\Delta V/V \approx 1 \cdot 10^{-3}$. The temperature range of this divergence is clearly visible in β which signals anomalous contributions to the volume changes up to ~ 75 K. As will be shown below, the anomalous length changes $\Delta L'_i = \Delta L_i - \Delta L_i^{\text{el,ph}}$ are strongly suppressed by external magnetic fields which suggests its magnetic nature. Short-range ferromagnetic correlations have been indeed detected in Eu_2CuSi_3 by electron spin resonance below $T \simeq 100$ K. [9] We conclude that the observed anomalous length changes are associated to ferromagnetic short range magnetic correlations.

The uniaxial length changes in Eu_2CuSi_3 along the a - and the c -axis, respectively, show pronounced anisotropy which is reflected by the fact that, well above the anomalies at $T = 150$ K, α_c is about three times larger than α_a (Fig. 1b). As in β , in both directions the onset of long range magnetic order is associated with clear anomalies. Interestingly, in both directions long range magnetic order is associated with shrinking of the respective lattice parameters a and c , i.e., positive uniaxial pressure dependence of T_C . In α_c , there is a peak at T_C followed by a broad hump centered around 15 K. In contrast, the anomalous contributions are much broader in α_a and there is only a rather jump-like anomaly at T_C . Upon further cooling, no additional hump can be identified. The structural changes are further illustrated by the distortion parameter $\delta = (L'_c - L'_a)/(L'_c + L'_a)$ and its derivative shown in Fig. 2. The data confirm that the ferromagnetic phase transition at T_C is associated with a kink in the distortion parameter and a large regime of structural fluctuations up to about 75 K. Upon cooling towards T_C , $\partial\delta/\partial T$ smoothly increases in a Curie-Weiss-like manner, i.e., as $C/(T + \Theta)$, with $\Theta \approx 27.5$ K. Note, that this description of the derivative of the parameter δ does not reflect the high-temperature mean-field approximation but only

phenomenologically describes the behavior upon approaching T_C . Just below T_C , $\partial\delta/\partial T$ is temperature independent, i.e., δ decreases linearly. A large hump of $\partial\delta/\partial T$ centered at 12 K is observed in the temperature regime below about 25 K. These distortions appear in the temperature regime where magnetic anisotropy starts to decrease through a spin reorientation process which finally yields vanishing anisotropy below $T \sim 5$ K. [9] To be specific, upon cooling magnetic moments rotate from the easy magnetic c -axis towards $\perp c$, thereby lifting the magnetic anisotropy. One may attribute the low temperature humps of the specific heat[9] and of $\partial\delta/\partial T$ as the thermodynamic signatures of this spin-reorientation towards the ab -plane.

In order to discuss the anomalous length changes in more detail, Fig. 3 presents the low temperature thermal expansion and the specific heat [1]. Again, the data have been corrected for the phononic and electronic contributions obtained from analysing of c_p of La_2CuSi_3 , yielding the magnetic contributions β' and α_i' . [1, 9] Different ordinate scales have been used to highlight the similarities and differences in the temperature dependencies. The data show that, at temperatures $\lesssim T_C$, the magnetic specific heat c_p^{magn} resembles quite well the volume thermal expansion coefficient β' while scaling fails at $T > T_C$ (Fig. 3a). At temperatures $T > T_C$, our data exclude similar temperature dependencies of β' and c_p^{magn} .

In the presence of one dominant energy scale ϵ of the respective ordering phenomenon, the scaling between c_p^{magn} and β' is described by the Grüneisen relation

$$\frac{\beta'}{c_p^{\text{magn}}} = \frac{1}{V} \left. \frac{\partial \ln \epsilon}{\partial p} \right|_T. \quad (3)$$

Applying Eq. 3 to the data in Fig. 3a yields the hydrostatic pressure dependence $\partial \ln \epsilon / \partial p = 13(2) \cdot 10^{-2} / \text{GPa}$ for the temperature range $T \leq T_C$ where c_p^{magn} scales to β' . Assuming ϵ being proportional to T_C , this yields $dT_C/dp_a = 4.4(9) \text{ K/GPa}$.

In contrast to the volume effect, there is no general Grüneisen scaling below T_C if the uniaxial pressure effects are considered. However, c_p^{magn} still fairly scales to both α_a' and α_c' in the reduced temperature regime $25 \text{ K} \leq T \leq T_C$ (see Fig. 3b). Here, the analysis yields $\partial \ln \epsilon / \partial p_a = 2.5(2) \cdot 10^{-2} / \text{GPa}$ and $\partial \ln \epsilon / \partial p_c = 8.0(9) \cdot 10^{-2} / \text{GPa}$ or $dT_C/dp_a = 0.85(10) \text{ K/GPa}$ and $dT_C/dp_c = 2.7(3) \text{ K/GPa}$, respectively. For both α_c' and α_a' , simple Grüneisen scaling can be excluded for $T \leq 25 \text{ K}$.

In general, one may identify three temperature regions with different behavior as indicated in Fig. 3: (1) At $T > T_C$, the anomalous volume changes as well as the uniaxial length

changes do not obey Grüneisen scaling. (2) Upon evolution of long range magnetic order at T_C , there is a rather temperature independent hydrostatic pressure dependence of ϵ down to 5 K. For the uniaxial pressure dependencies, this regime is restricted to $T_{\text{SR}}^{\text{onset}} \leq T \leq T_C$. (3) Below $T_{\text{SR}}^{\text{onset}}$, where the distortion parameter δ signals spin reorientation, the uniaxial pressure dependencies for pressure applied along the a - and c -axis, respectively, strongly differ.

EFFECT OF EXTERNAL MAGNETIC FIELDS

Figures 4 and 5 show the effect of external magnetic fields on the uniaxial length changes. Magnetic fields up to 15 T affect the lengths changes well above T_C indicating structural changes up to ~ 80 K for $B \parallel c$ and ~ 200 K for $B \parallel a$. While the a -axis shrinks in external magnetic field in the entire temperature range up to 200 K, the c -axis displays a heterogeneous response and anomalous magnetostriction is restricted to $T < 100$ K. Upon application of $B = 15$ T, the c -axis overall shrinks above $T \simeq 60$ K while it strongly increases below. As will be discussed in more detail below, there is a sign change of the magnetostriction coefficient $\lambda_c(B)$ at $T_C < T \lesssim 75$ K.

The field effect on the anomaly at $T_C = 34$ K is most visible if the thermal expansion coefficients in Fig. 5 are considered. Both α_a and α_c show a broadening of the anomaly at T_C in external magnetic field. The ferromagnetic nature of the phase transition is reflected by the strong shift of anomalous length changes to higher temperatures and the sharp anomalies observed at $B = 0$ are not observed in finite magnetic field. In magnetic fields $B \geq 5$ T, no clear anomaly can be observed anymore. Even in finite fields $B < 5$ T, the λ -like peak in α_a which is the most distinct signature of the phase transition smears out and converts into a jump-like feature. We hence consider the middle of this jump being a relevant signature for the evolution of ferromagnetic correlations. Together with all other features extracted from the data as described in the following, it is used to construct the magnetic phase diagram in Fig. 8. In contrast to the anomaly at T_C , the low-temperature hump indicative of spin-reorientation from the c -axis into the ab -plane is suppressed in external magnetic fields. This is straightforwardly attributed to the fact that the spin reorientation towards $\perp c$ is hindered by $B \parallel c$. We define this spin-reorientation regime using the concave kink in the curve, and the convex kink is used to define the crossover to isotropic magnetic behavior,

marked by the black arrows in Fig. 5a. For fields larger than 10 T, α_c becomes negative at low temperature and the features signaling spin-reorientation are not observed in the temperature regime under study. In the ab -plane, the effects of magnetic fields on α are quite different. The anomaly at T_C is smeared out as well, but a clear maximum remains observable even in fields up to $B = 15$ T where a kink is seen in α_a at $T \approx 32$ K.

These differences associated with the actual direction of the magnetic field with respect to the crystallographic axes are also seen in the linear magnetostriction coefficients λ_c and λ_a displayed in Fig. 7. In the ab -plane, λ is negative at all fields and temperatures under study. At $T = 5$ K, there are two anomalies as indicated by arrows in Fig. 7b. One of which is associated with a peak at $B = 0.5$ T and the other with a kink at $B = 4.5$ T. The position of the peak does not change upon heating up to 15 K, appears at a slightly reduced field at $T = 31.5$ K and disappears above T_C . A very similar behavior with however opposite sign is found in λ_a which shows a peak maximum at low field. Above T_C , the minimum in λ_a converts into a kink where the slope of λ_a changes. This kink becomes more and more broad upon heating. Correspondingly, there is a minimum in λ_c above T_C which is shifted to higher fields upon heating. At $T = 50$ K, there is still a broad anomaly centered around $B = 1.5$ T. Both features observed above T_C display the same B vs. T behavior (see Fig. 8) so that we conclude a common nature. In contrast, the above mentioned kink in λ_a is restricted $T \leq T_{SR}$. The nonuniform response of the length changes for $B \parallel c$ are displayed by the magnetostriction coefficients obtained at $T_C \leq T < 100$ K. Associated with the minimum discussed above, magnetostriction is negative at low fields and positive at high magnetic fields.

DISCUSSION AND CONCLUSIONS

The onset of long range magnetic order yields shrinking of the sample both along the c - and the a -direction. Eu_2CuSi_3 displays stable valence of Eu^{2+} below room temperature. Its $4f^7$ electronic configuration implies no orbital momentum and the Steven's factors vanish so that magnetic anisotropy and magnetoelastic effects induced by spin-orbit coupling is negligible. In the half-filled shell, crystal field effects can be excluded either. We also note, that the observed anomalous length changes are not associated with unstable Eu valence. [19] The strong magnetoelastic effect might result from either dipole-dipole interaction or anisotropic

magnetic coupling. Above T_C , both α_c and α_a imply the presence of anomalous length changes at elevated temperatures up to ~ 80 K, i.e., far above the Curie temperature. We attribute these anomalous length changes to the presence of ferromagnetic correlations. In this temperature regime, the evolution of short range ferromagnetic order is associated with a structural distortion, i.e., finite distortion parameter δ . Recent ESR data suggest that the effective internal field in the short-range-correlated region is parallel to the c -axis. [9] Noteworthy, Grüneisen scaling does not apply in this temperature regime. Due to the fact that the Grüneisen parameter obtained in the long-range ordered phase does not describe the relation between β' and c_p^{magn} at $T > T_C$, one has to conclude the different nature of short range and long range magnetic order. In particular, the failure of simple Grüneisen scaling at $T_C < T \leq 50$ K suggests competing ordering phenomena in this temperature regime.

This is corroborated by the observed anisotropic field dependencies at high temperatures. In general, both magnetic fields $\parallel c$ and $\perp c$ stabilize the ferromagnetic correlations and there is a pronounced magnetic field dependence. Upon application of magnetic fields $B \parallel c$, the sharp thermodynamic signature of long-range magnetic order at T_C disappears and strongly smears out already in small magnetic field. Although this is a typical behaviour for ferromagnets where no true magnetic phase transition appears in finite magnetic field, we note that our data do not unambiguously prove long range order at $B \parallel c \geq 0.5$ T. The data for $B \perp c$ do not clarify this issue either, as the jump-like feature in α_a disappears in magnetic field. However, in contrast to the case $B \parallel c$, the maximum in α_a is not significantly affected as indicated by the vertical dashed line in Fig. 8. The phase boundary evidenced by the magnetostriction data at $B \sim 0.4$ T might hence either indicate melting of (true) long-range order or the stabilisation of a competing ordered phase. A spin-flop nature of this phase boundary can be excluded because it is observed in both field directions as well as above and within the spin-reoriented phase. The origin of the feature at around 4.5 T and $T < T_{\text{SR}}$ is unknown. The fact that T_{SR} and the associated onset temperature are suppressed by $B \parallel c$ support the scenario that, at T_{SR} , reorientation of the magnetic moments from $\parallel c$ towards the ab -plane appears. For $B \parallel a$, the data do not allow to extract T_{SR} .

Despite the easy c -axis nature of long range order in Eu_2CuSi_3 , magnetic fields $B \parallel c$ do stabilize the short range magnetic order less than $B \perp c$. This observation supports our conclusion that the nature of short range order differs from the magnetically ordered state.

Our observation of magnetostrictive effects even at 200 K straightforwardly connects to the anomalous magnetoresistance in Eu_2CuSi_3 . [7, 9] Upon application of $B = 6$ T, negative magnetoresistive has been observed up to about 80 K for $B \parallel c$ and about 130 K for $B \perp c$. [9] On the one hand, structural changes proven by our high-precision dilatometry data presented here naturally explain associated changes of the electric transport properties. Quantitatively, the larger magnetoresistance for $B \perp c$ observed in the experiment can be explained by the anisotropic effect of magnetic field on the structure, i.e., stronger magnetostrictive effects for $B \perp c$.

In summary, we have studied the thermodynamic properties and their field dependence of intermetallic single crystalline Eu_2CuSi_3 . At the ferromagnetic ordering temperature, strong magnetostrictive coupling yields a pronounced λ -like anomaly in the thermal expansion coefficient. The distortion parameter signals short-range order far above T_C . A spin-reorientation regime as well as a non-uniform energy scale are indicated by Grüneisen analysis of the data at low temperatures. The magnetic field effect both on the long-range order, the spin-reorientation, and the short-range order is highly anisotropic and yields anomalous magnetostrictive effects up to about 200 K.

RK gratefully acknowledges fellowship of the Marsilius Kolleg Heidelberg. CDC acknowledges financial support by the National Natural Science Foundation of China Grant No. 51471135, the National Key Research and Development Program of China under contract No. 2016YFB1100101, and Shaanxi International Cooperation Program.

* Email: l.wang@kip.uni-heidelberg.de

- [1] J. S. Hwang, K. Lin, and C. Tien, Solid State Communications **100**, 169 (1996), ISSN 0038-1098, URL <http://www.sciencedirect.com/science/article/pii/0038109896003808>.
- [2] C. Tien, L. Luo, and J. S. Hwang, Phys. Rev. B **56**, 11710 (1997), URL <http://link.aps.org/doi/10.1103/PhysRevB.56.11710>.
- [3] C. Tien and L. Luo, Solid State Communications **107**, 295 (1998), ISSN 0038-1098, URL <http://www.sciencedirect.com/science/article/pii/S0038109898002270>.
- [4] G. Nakamoto, Y. Shibai, M. Kurisu, and Y. Andoh, Physica B: Condensed Matter **281-282**, 76 (2000), ISSN 0921-4526, URL

- <http://www.sciencedirect.com/science/article/pii/S0921452699010868>.
- [5] D. Li, Y. Shiokawa, S. Nimori, Y. Haga, E. Yamamoto, T. Matsuda, and Y. Onuki, *Physica B: Condensed Matter* **329-333**, Part 2, 506 (2003), ISSN 0921-4526, proceedings of the 23rd International Conference on Low Temperature Physics, URL <http://www.sciencedirect.com/science/article/pii/S0921452602021750>.
 - [6] D. Li, X. Zhao, and S. Nimori, *Journal of Physics: Condensed Matter* **21**, 026006 (2009), URL <http://stacks.iop.org/0953-8984/21/i=2/a=026006>.
 - [7] S. Majumdar, R. Mallik, E. V. Sampathkumaran, K. Rupprecht, and G. Wortmann, *Phys. Rev. B* **60**, 6770 (1999), URL <http://link.aps.org/doi/10.1103/PhysRevB.60.6770>.
 - [8] C. D. Cao, R. Klingeler, N. Leps, H. Vinzelberg, V. Kataev, F. Muranyi, N. Tris-tan, A. Teresiak, S. Zhou, W. Löser, et al., *Phys. Rev. B* **78**, 064409 (2008), URL <http://link.aps.org/doi/10.1103/PhysRevB.78.064409>.
 - [9] C. D. Cao, R. Klingeler, H. Vinzelberg, N. Leps, W. Löser, G. Behr, F. Mu-ranyi, V. Kataev, and B. Büchner, *Phys. Rev. B* **82**, 134446 (2010), URL <http://link.aps.org/doi/10.1103/PhysRevB.82.134446>.
 - [10] Y. Zhang, D. Guo, Y. Yang, S. Geng, X. Li, Z. Ren, and G. Wilde, *Journal of Alloys and Compounds* (in print) pp. – (2017), ISSN 0925-8388, URL <http://www.sciencedirect.com/science/article/pii/S0925838817303390>.
 - [11] A. Raman, *Naturwissenschaften* **54**, 560 (1967).
 - [12] C. Cao, W. Löser, G. Behr, R. Klingeler, N. Leps, H. Vinzelberg, and B. Büchner, *Journal of Crystal Growth* **318**, 1043 (2011), ISSN 0022-0248, the 16th International Conference on Crystal Growth (ICCG16)/The 14th International Conference on Vapor Growth and Epitaxy (ICVGE14), URL <http://www.sciencedirect.com/science/article/pii/S0022024810009577>.
 - [13] R. Mallik, E. Sampathkumaran, M. Strecker, G. Wortmann, P. Paulose, and Y. Ueda, *Journal of Magnetism and Magnetic Materials* **185**, L135 (1998), ISSN 0304-8853, URL <http://www.sciencedirect.com/science/article/pii/S0304885398001243>.
 - [14] M. Schneider, A. Gladun, A. Kreyssig, J. Wosnitza, D. Souptel, and G. Behr, *Journal of Magnetism and Magnetic Materials* **311**, 489 (2007), ISSN 0304-8853, URL <http://www.sciencedirect.com/science/article/pii/S0304885306009851>.
 - [15] A. del Moral, J. I. Arnaud, M. R. Ibarra, J. S. Abell, and E. W. Lee, *Journal of Physics C: Solid State Physics* **19**, 579 (1986), URL

- <http://stacks.iop.org/0022-3719/19/i=4/a=018>.
- [16] H. Zhao, M. Kramer, and M. Akinc, *Intermetallics* **12**, 493 (2004), ISSN 0966-9795, URL <http://www.sciencedirect.com/science/article/pii/S0966979504000275>.
 - [17] L. Wang, U. Köhler, N. Leps, A. Kondrat, M. Nale, A. Gasparini, A. de Visser, G. Behr, C. Hess, R. Klingeler, et al., *Phys. Rev. B* **80**, 094512 (2009), URL <http://link.aps.org/doi/10.1103/PhysRevB.80.094512>.
 - [18] E. Gratz and A. Lindbaum, *Journal of Magnetism and Magnetic Materials* **137**, 115 (1994), ISSN 0304-8853, URL <http://www.sciencedirect.com/science/article/pii/0304885394901953>.
 - [19] G. Neumann, J. Langen, H. Zahel, D. Plümacher, Z. Kletowski, W. Schlabit, and D. Wohlleben, *Zeitschrift für Physik B Condensed Matter* **59**, 133 (1985), ISSN 1431-584X, URL <http://dx.doi.org/10.1007/BF01725529>.
 - [20] Note, that our analysis of c_p of La_2CuSi_3 applying the Debye function up to 50 K yield a different value for Θ_D as compared to the T^3 -law fitting used in Ref. 1. The obtained $\Theta_D = 445$ K was renormalised in order to account for the different masses.

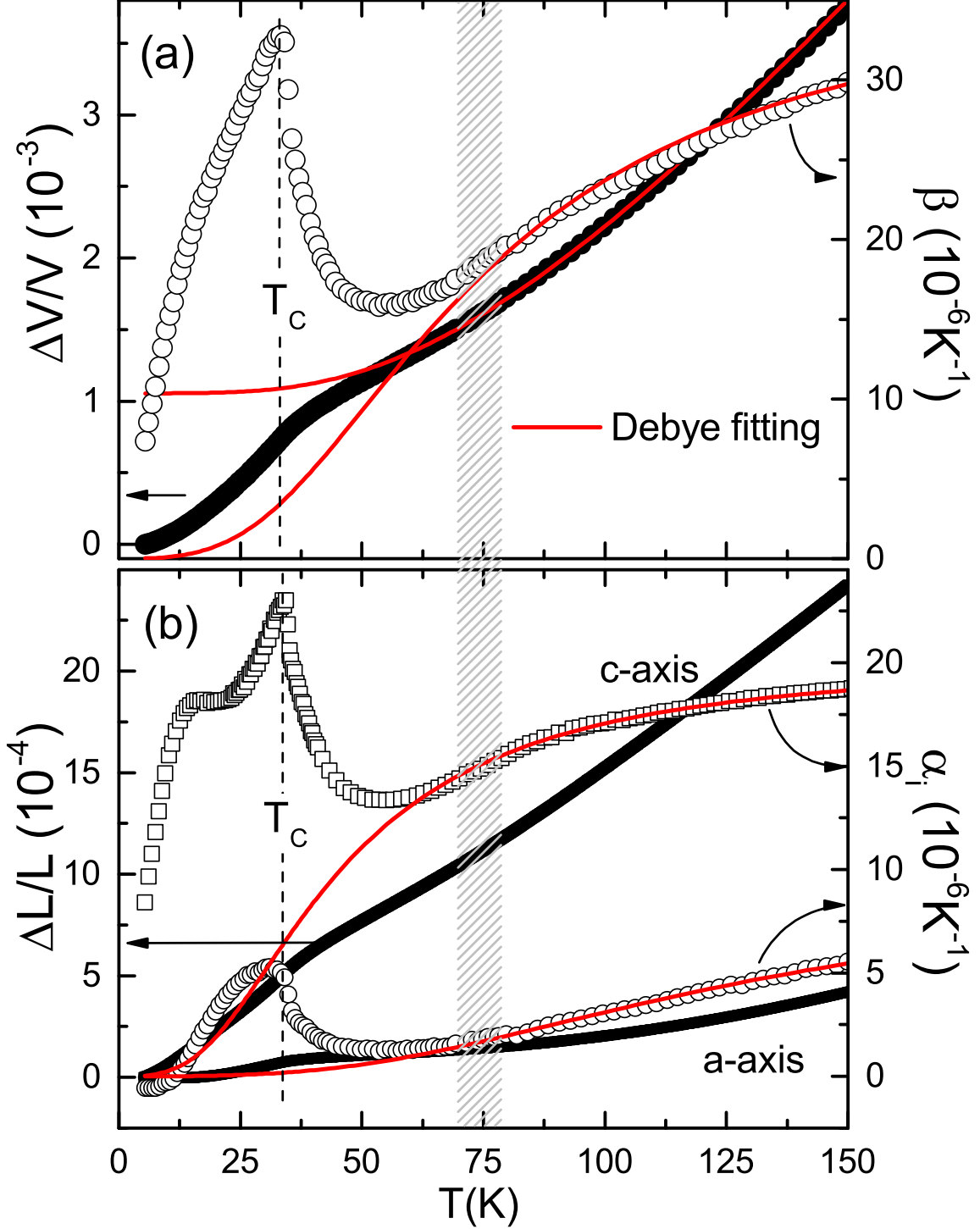


FIG. 1: (a) Relative volume changes $\Delta V/V$ (left ordinate) and volume thermal expansion coefficient β of Eu_2CuSi_3 vs. temperature T . T_C denotes the Curie temperature at which the Eu-moments order ferromagnetically. The red lines are a Debye fit to the data well above T_C (see the text). (b) Relative length changes $\Delta L/L$ (left ordinate) and linear thermal expansion coefficients α of Eu_2CuSi_3 measured within the a/b -plane (circles) and along the c -axis (squares) vs. temperature T .

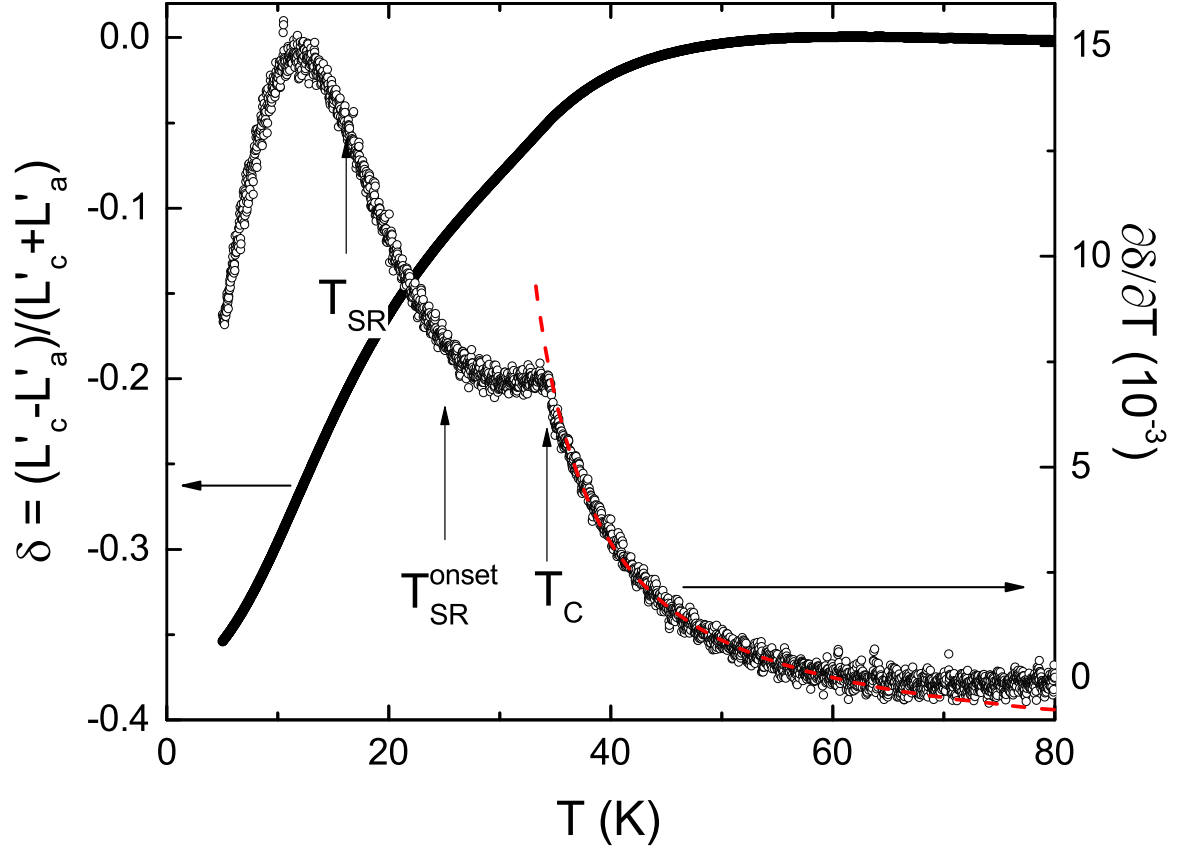


FIG. 2: Distortion parameter δ and its derivative as derived from the anomalous lengths changes $\Delta L'_i$. T_{SR} indicates the spin reorientation temperature. The dashed line is a phenomenological Curie-Weiss fit to the data.

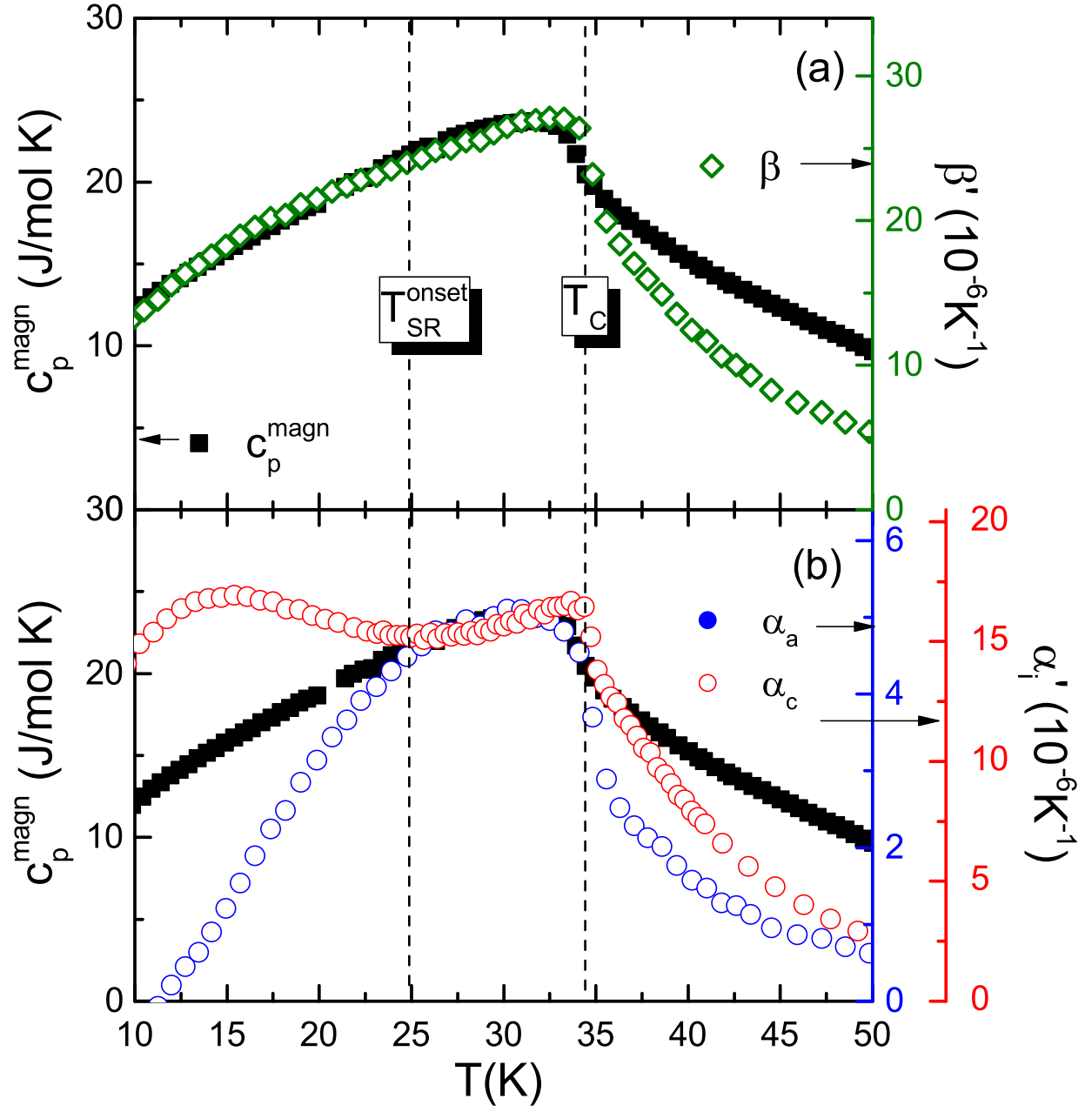


FIG. 3: (a) Anomalous volume thermal expansion coefficient β' and magnetic specific heat c_p^{magn} illustrating Grüneisen scaling in Eu_2CuSi_3 . (b) Anomalous linear thermal expansion coefficients α_a' and α_c' , and c_p^{magn} .

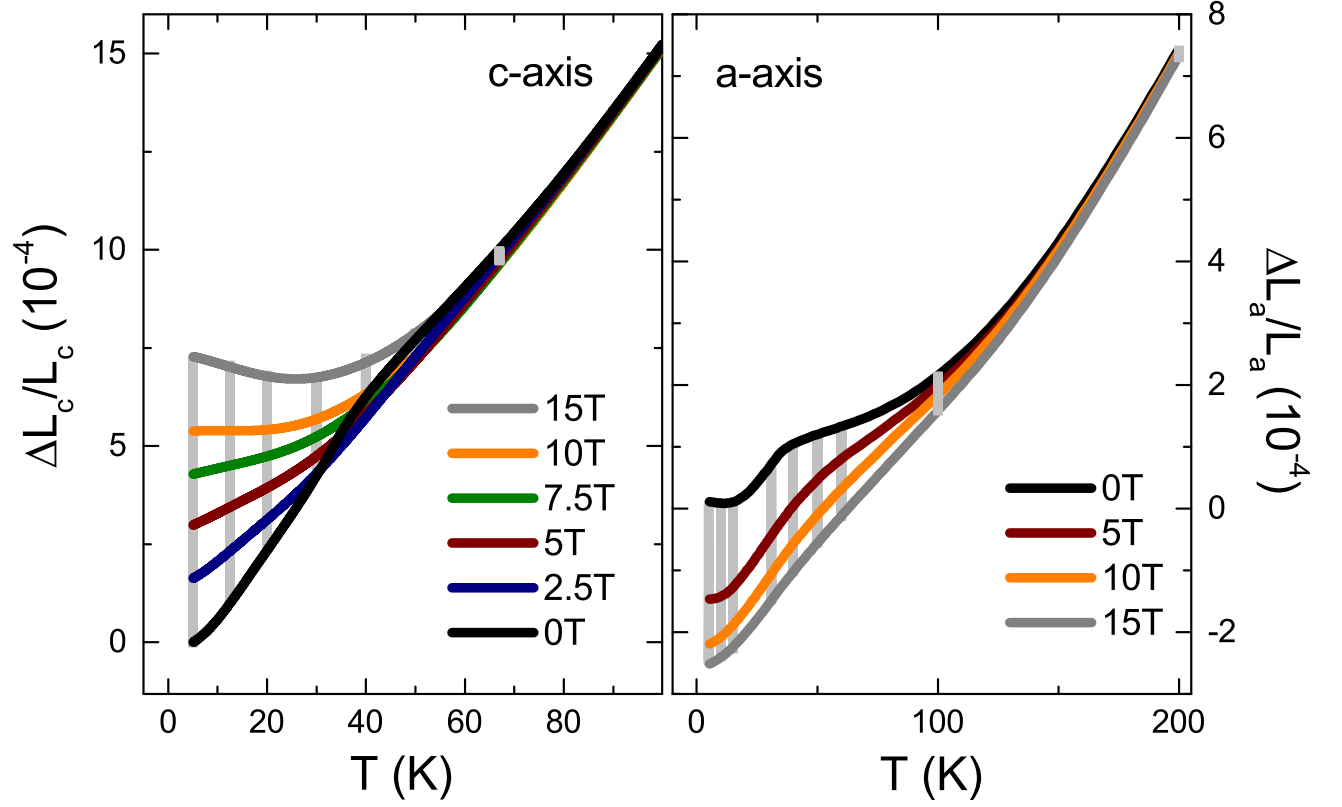


FIG. 4: Relative length changes $\Delta L/L$ in different external magnetic fields vs. temperature measured along the c - and a -axis, respectively. The data at $B \neq 0$ have been shifted according to the measured magnetostriction at 5 K. The grey vertical lines show the measured magnetostriction up to 15 T at various temperatures (see Fig. 6).

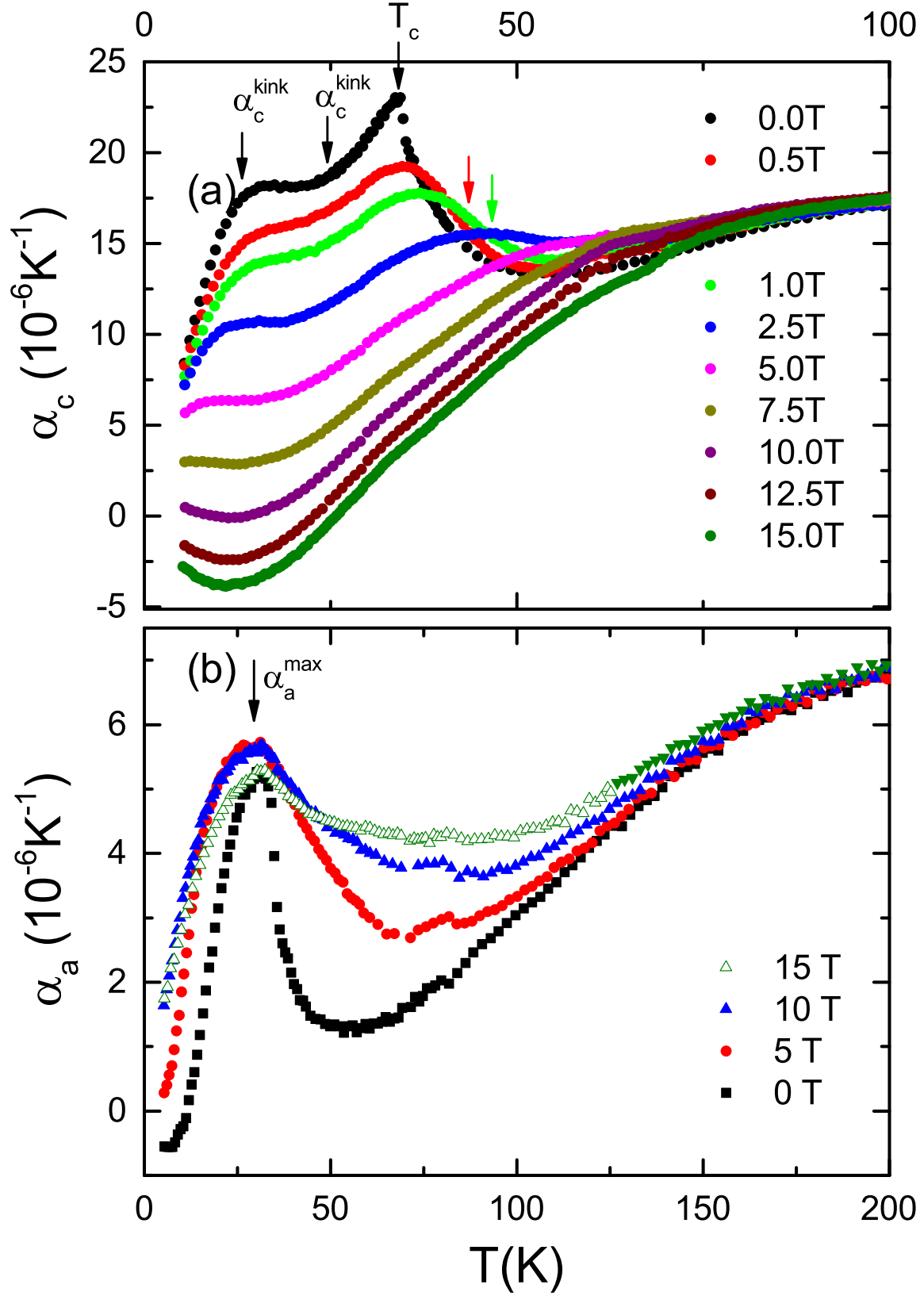


FIG. 5: Linear thermal expansion coefficients α_c (a) and α_a (b) of Eu_2CuSi_3 in different external magnetic fields applied in the direction of measurements. Arrows indicate anomalies as discussed in the text.

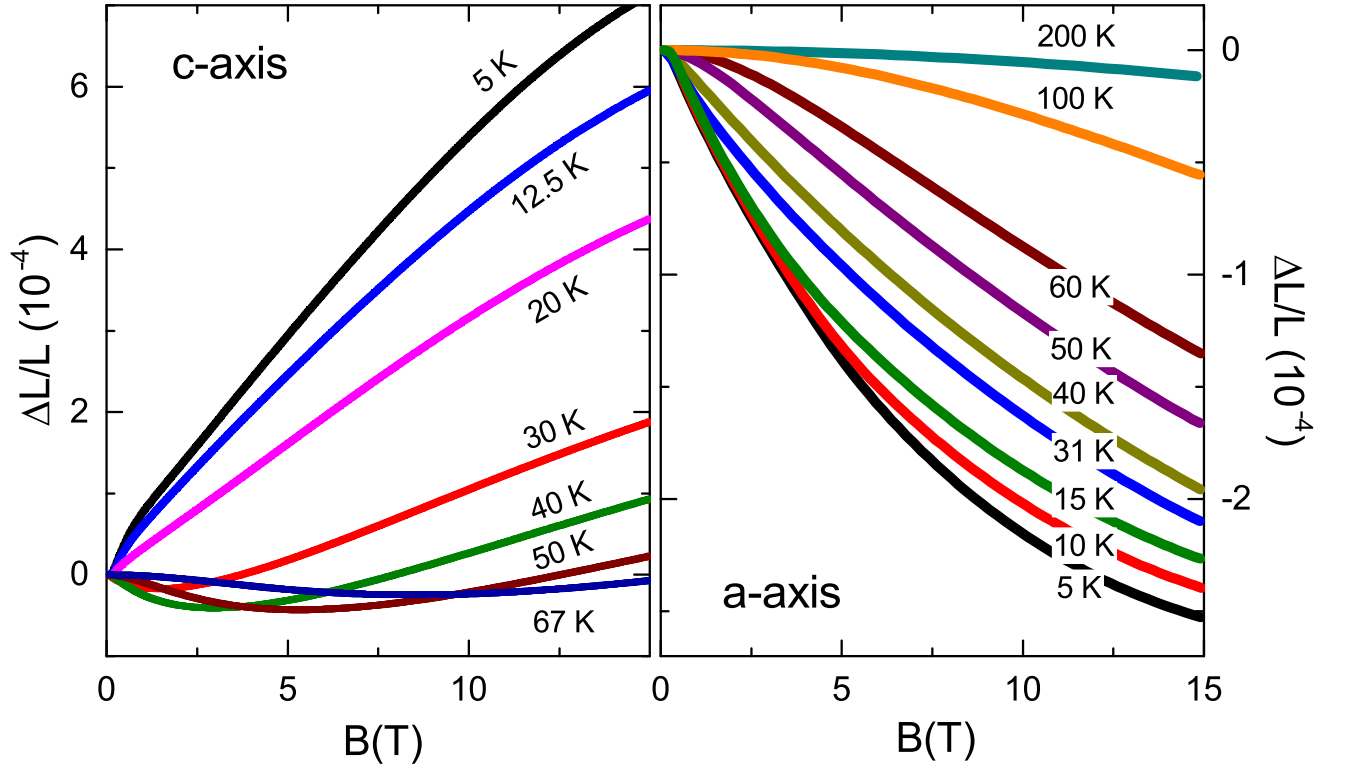


FIG. 6: Magnetostriction $\Delta L/L$ at different temperatures measured along the c - and a -axis, respectively.

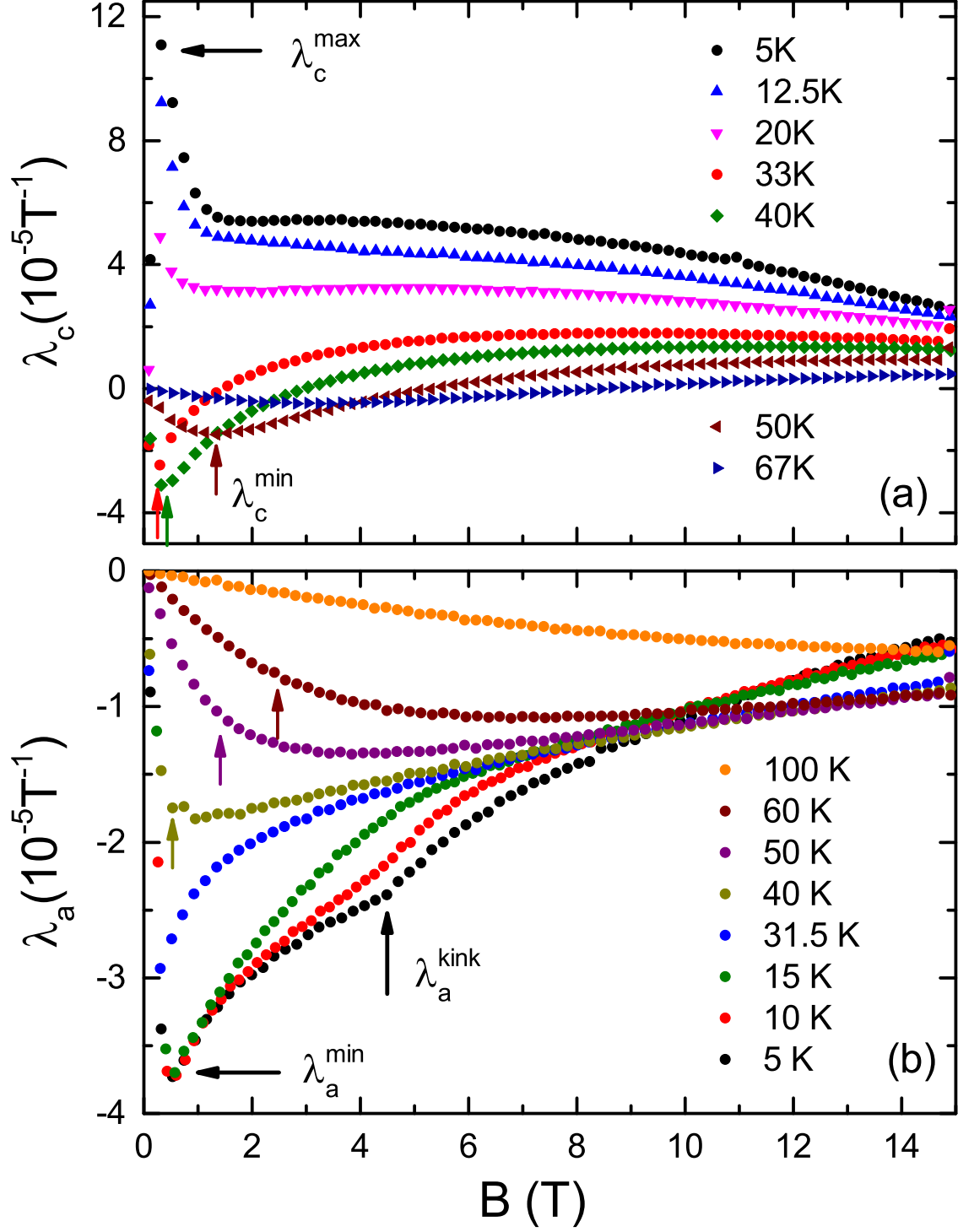


FIG. 7: (a) Linear magnetostriction coefficients λ_c (a) and λ_a (b) of Eu_2CuSi_3 at different temperatures. The arrows highlight anomalies discussed in the text.

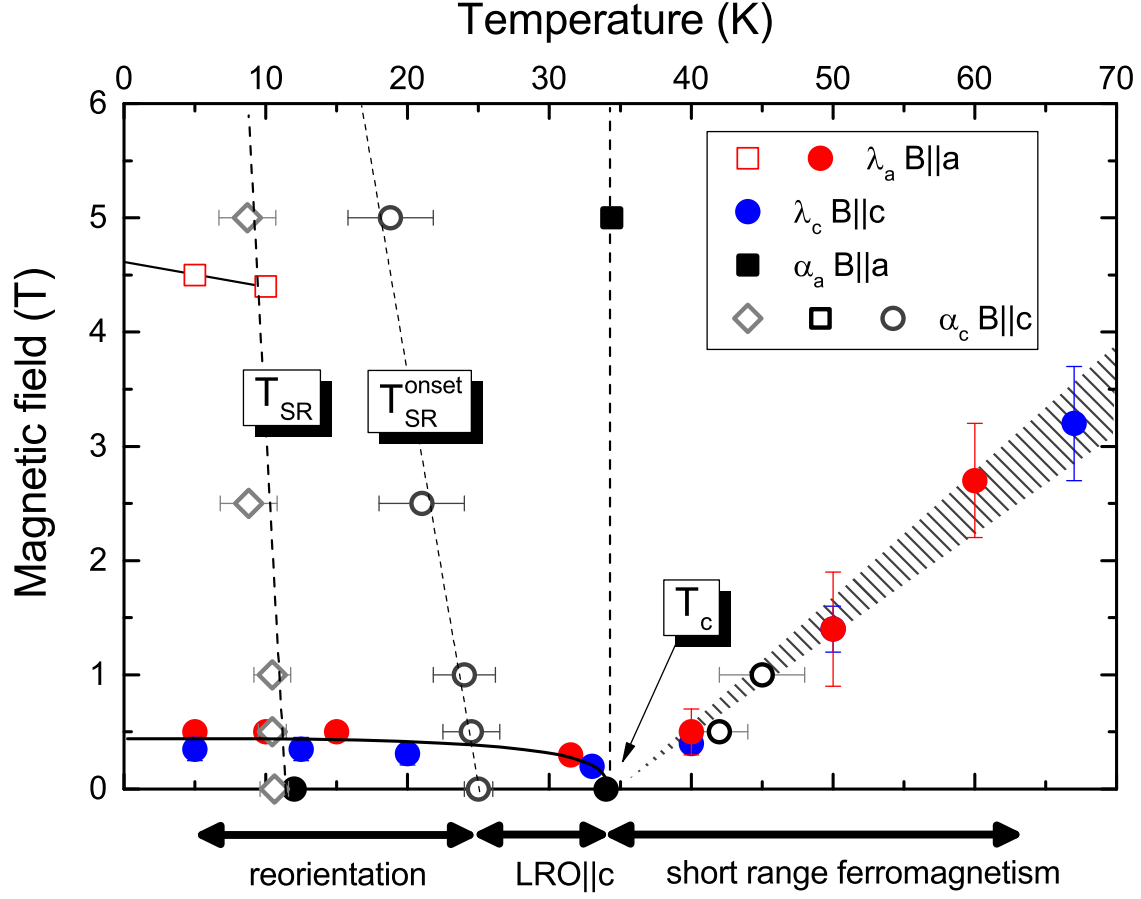


FIG. 8: Magnetic phase diagram of Eu_2CuSi_3 . Color symbols (red & blue) are deduced from the magnetostriction λ_i , black symbols (solid & hollow) are from the temperature dependent length changes α_i at different magnetic fields. The black arrows below the graph illustrate regions of different magnetic behaviour at $B = 0$. The dashed and shaded lines are guides to the eye indicating the evolution of ferromagnetism and spin reorientation.